



Universiteit  
Leiden  
The Netherlands

## **von Hippel-Lindau tumor suppressor mutants faithfully model pathological hypoxia-driven angiogenesis and vascular retinopathies in zebrafish**

Rooijen, E. van; Voest, E.E.; Logister, I.; Bussmann, J.; Korving, J.; Eeden, F.J. van; ... ; Schulte-Merker, S.

### **Citation**

Rooijen, E. van, Voest, E. E., Logister, I., Bussmann, J., Korving, J., Eeden, F. J. van, ... Schulte-Merker, S. (2010). von Hippel-Lindau tumor suppressor mutants faithfully model pathological hypoxia-driven angiogenesis and vascular retinopathies in zebrafish. *Disease Models And Mechanisms*, 3, 343-353. doi:10.1242/dmm.004036

Version: Not Applicable (or Unknown)  
License: [Leiden University Non-exclusive license](#)  
Downloaded from: <https://hdl.handle.net/1887/61777>

**Note:** To cite this publication please use the final published version (if applicable).

# von Hippel-Lindau tumor suppressor mutants faithfully model pathological hypoxia-driven angiogenesis and vascular retinopathies in zebrafish

Ellen van Rooijen<sup>1,2</sup>, Emile E. Voest<sup>2</sup>, Ive Logister<sup>1,2</sup>, Jeroen Bussmann<sup>1</sup>, Jeroen Korving<sup>1</sup>, Fredericus J. van Eeden<sup>3</sup>, Rachel H. Giles<sup>2</sup> and Stefan Schulte-Merker<sup>1,\*</sup>

## SUMMARY

Biallelic inactivation of the von Hippel-Lindau (VHL) tumor suppressor gene predisposes human patients to the development of highly vascularized neoplasms in multiple organ systems. We show that zebrafish *vhl* mutants display a marked increase in blood vessel formation throughout the embryo, starting at 2 days post-fertilization. The most severe neovascularization is observed in distinct areas that overlap with high *vegfa* mRNA expression, including the *vhl* mutant brain and eye. Real-time quantitative PCR revealed increased expression of the duplicated *VEGFA* orthologs *vegfaa* and *vegfab*, and of *vegfb* and its receptors *flt1*, *kdr* and *kdr-like*, indicating increased vascular endothelial growth factor (Vegf) signaling in *vhl* mutants. Similar to VHL-associated retinal neoplasms, diabetic retinopathy and age-related macular degeneration, we show, by tetramethyl rhodamine-dextran angiography, that vascular abnormalities in the *vhl*<sup>-/-</sup> retina lead to vascular leakage, severe macular edema and retinal detachment. Significantly, vessels in the brain and eye express *cxcr4a*, a marker gene expressed by tumor and vascular cells in VHL-associated hemangioblastomas and renal cell carcinomas. VEGF receptor (VEGFR) tyrosine kinase inhibition (through exposure to sunitinib and 676475) blocked *vhl*<sup>-/-</sup>-induced angiogenesis in all affected tissues, demonstrating that Vegfaa, Vegfab and Vegfb are key effectors of the *vhl*<sup>-/-</sup> angiogenic phenotype through Flt1, Kdr and Kdr-like signaling. Since we show that the *vhl*<sup>-/-</sup> angiogenic phenotype shares distinct characteristics with VHL-associated vascular neoplasms, zebrafish *vhl* mutants provide a valuable in vivo vertebrate model to elucidate underlying mechanisms contributing to the development of these lesions. Furthermore, *vhl* mutant zebrafish embryos carrying blood vessel-specific transgenes represent a unique and clinically relevant model for tissue-specific, hypoxia-induced pathological angiogenesis and vascular retinopathies. Importantly, they will allow for a cost-effective, non-invasive and efficient way to screen for novel pharmacological agents and combinatorial treatments.

## INTRODUCTION

Blood vessel formation is a dynamic process that is tightly regulated to ensure oxygen homeostasis in vertebrates. During embryogenesis, this involves the de novo formation of blood vessels by differentiation of endothelial precursors, or angioblasts, to form the primary vascular network (vasculogenesis), and the formation of new blood vessels that branch off from existing vessels (angiogenesis or neovascularization) (Carmeliet, 2000). Adult blood vessels are normally quiescent unless the balance of angiogenic inhibitors is tipped in favor of angiogenic activators (termed 'angiogenic switch') during normal physiological processes, such as in wound healing or during the female reproductive cycle (Carmeliet, 2000). Angiogenesis is also crucial for the pathological progression of tumor growth and angiogenesis-related disorders, including many retinopathies that lead to vision loss (Arjamaa and Nikinmaa, 2006), such as age-related macular degeneration and diabetic retinopathies.

The hypoxia-induced transcription factor (HIF) is perceived as the master transcriptional regulator of hypoxia-inducible genes that are involved in adaptive cellular responses to oxygen (Kaelin, 2005),

including those genes that are involved in angiogenesis (reviewed in Pugh and Ratcliffe, 2003; Liao and Johnson, 2007; Dewhirst et al., 2008). HIF is a heterodimer composed of a hypoxia-regulated alpha subunit (HIF-1 $\alpha$ , HIF-2 $\alpha$  or HIF-3 $\alpha$ ), and an oxygen-insensitive HIF-1 $\beta$  subunit (also known as the aryl hydrocarbon receptor nuclear translocator, or ARNT) (Semenza, 2001). Under normoxic conditions, HIF- $\alpha$  is hydroxylated on either of two prolyl residues by the family of prolyl hydroxylases (PHD1-3), and targeted for rapid proteasomal degradation by a multi-subunit E3 ubiquitin ligase complex, containing the von Hippel-Lindau (VHL) protein as the substrate recognition component. In the absence of oxygen or functional pVHL (the VHL gene product), HIF- $\alpha$  protein is stabilized and translocated to the nucleus where it partners with HIF- $\beta$  to form functional HIF, triggering an increased expression of multiple angiogenic growth factors (Pugh and Ratcliffe, 2003), including vascular endothelial growth factor (VEGF, or VEGFA) (Liu et al., 1995; Forsythe et al., 1996), plasminogen activator inhibitor-1 (PAI-1) (Kietzmann et al., 1999), angiopoietin-2 (ANG-2) (Oh et al., 1999), platelet-derived growth factor (PDGF) (Gleadle et al., 1995), stromal-derived factor-1 (SDF-1, or CXCL12) and CXC chemokine receptor 4 (CXCR4) (Kryczek et al., 2005).

The secreted glycoprotein VEGFA is regarded as the key regulator of both physiological and pathophysiological angiogenesis as it facilitates blood vessel growth and remodeling processes by increasing vascular permeability and changing the extravascular matrix. Additionally, VEGFA provides mitogenic and survival stimuli for endothelial cells (reviewed in Thomas, 1996;

<sup>1</sup>Hubrecht Institute, Royal Netherlands Academy of Arts and Sciences (KNAW) and University Medical Center Utrecht, 3584 CT Utrecht, The Netherlands

<sup>2</sup>Department of Medical Oncology, University Medical Center Utrecht, 3584 CG Utrecht, The Netherlands

<sup>3</sup>Department of Biomedical Science, Sheffield University, Western Bank, Sheffield S10 2TN, United Kingdom

\*Author for correspondence (s.schulte@hubrecht.eu.)

Yancopoulos et al., 2000; Carmeliet, 2005). Recently, it was shown that autocrine VEGFA signaling is also required for vascular homeostasis (Lee et al., 2007). VEGFA acts through two high affinity receptor tyrosine kinases, FLT-1 (VEGFR1) and KDR (VEGFR2 or Flk-1). KDR is thought to mediate most of the angiogenic functions of VEGFA, whereas FLT1 may act as a sink for VEGFA, or as a decoy receptor to negatively regulate signaling through KDR (Yancopoulos et al., 2000).

Overproduction of hypoxia-inducible mRNAs, including VEGFA, is a hallmark of the highly vascularized neoplasms associated with biallelic inactivation of the VHL tumor suppressor gene, including hemangioblastomas of the retina and central nervous system (CNS), and clear cell renal cell carcinoma (ccRCC) (Maher et al., 1991; Maher and Kaelin, 1997; Van Poppel et al., 2000; Lonser et al., 2003). Hemangioblastomas are the most common manifestation of VHL disease, affecting 60-80% of all patients, and frequently causing neurological morbidity and mortality (Wanebo et al., 2003; Chew, 2005). These cystic tumors contain many thin-walled blood vessels that are separated by non-invasive neoplastic VHL<sup>-/-</sup> stromal cells (Vortmeyer et al., 1997), which were shown to be embryonically arrested hemangioblasts that express brachyury, KDR and the stem cell leukemia factor (SCL) (Park et al., 2007). Besides retinal hemangioblastomas, VHL patients can develop retinal neovascularization that is similar to diabetic retinopathy (Chew, 2005). Although activated HIF is a major contributor to the vascularization phenotype of VHL-associated neoplasms, pVHL appears to be essential for endothelial extracellular fibronectin matrix deposition in a HIF-independent fashion (Ohh et al., 1998; Bluysen et al., 2004; Tang et al., 2006). Furthermore, it has been shown that endothelial cells require pVHL for correct vascular patterning and maintenance of vascular integrity during development (Tang et al., 2006).

We recently reported that zebrafish (*Danio rerio*) with mutations in the VHL ortholog *vhl* display general hypoxic physiology, including the upregulation of hypoxia-induced genes, and a severe hyperventilation and cardiophysiological response (van Rooijen et al., 2009). Furthermore, *vhl* mutants have severe hematopoietic defects, closely resembling the human VHL-associated disorder Chuvash polycythemia.

Here, we investigate the effect of *vhl* loss on blood vessel formation. The zebrafish vascular system shows a remarkable functional conservation with humans (Vogel and Weinstein, 2000; Isogai et al., 2001; Zon and Peterson, 2005; Covassin et al., 2006). This has also been demonstrated in a pathological context, as tumor cells excreting human VEGFA strongly promoted zebrafish vessel remodeling and angiogenesis (Stoletov et al., 2007). Furthermore, the VEGF signaling pathway is highly conserved. Like all vertebrates, with the exception of placental mammals, zebrafish have four Vegf receptors (Flt1, Kdr, Kdr-like and Flt4); Kdr-like (also known as Kdr1) was lost during the evolution of placental mammals (Bussmann et al., 2007; Bussmann et al., 2008). Although Kdr and Kdr-like represent separate classes of Vegf receptor, the duplicated VEGFA orthologs Vegfaa and Vegfab can bind to, and activate, both receptors in vitro (Bahary et al., 2007).

Using blood vessel-specific transgenes, we show severe neovascularization of the *vhl*<sup>-/-</sup> brain, eye and trunk. We observed vascular leakage in the *vhl*<sup>-/-</sup> retina that results in severe macular edema and retinal detachment, resembling VHL-associated

vascular neoplasms and diabetic retinopathies. Quantitative real-time PCR (qPCR) indicates that there is increased Flt1, Kdr and Kdr-like signaling in *vhl* mutants. Treatment with VEGFR tyrosine kinase inhibitors that are used in the cancer clinic halted excess blood vessel formation, demonstrating that Vegfaa/b and Vegfb act as key effectors of the *vhl*<sup>-/-</sup> angiogenic phenotype by signaling through the Flt1, Kdr and Kdr-like receptors. We validate zebrafish *vhl* mutants as an important new in vivo model for pathological angiogenesis and vascular retinopathies.

## RESULTS

### *vhl* mutants display increased Flt1, Kdr and Kdr-like signaling

Through HIF- $\alpha$ , VHL plays a crucial role in the adaptive cellular response to hypoxia, including the regulation of angiogenesis through factors such as VEGFA. We have previously shown that *vhl* loss-of-function mutants display a systemic hypoxic response, including the upregulation of several angiogenesis-related genes (van Rooijen et al., 2009). At around 7.5 days-post fertilization (dpf), whole-mount in situ hybridization results revealed an overexpression of *vegfa* (*vegfaa*) mRNA, predominantly in the *vhl* mutant brain, eye and glomerulus. Increased *kdr* and *kdr-like* (also known as *kdr1*) mRNA expression was observed in blood vessels, the liver and the glomerulus. Additionally, *kdr* was expressed highly in the *vhl*<sup>-/-</sup> eye.

Here, we investigated the contribution of other Vegf signaling pathway components by qPCR. We identified the vertebrate VEGF ligands and performed synteny analyses using the Ensembl database (<http://www.ensembl.org>). We constructed a rooted neighbor-joining phylogenetic tree (Fig. 1A) showing the conservation of VEGF ligands in zebrafish. The duplicated zebrafish VEGFA orthologs *vegfaa* and *vegfab* (Bahary et al., 2007), as well as zebrafish *vegfc* (Ober et al., 2004) and *vegfd* (Song et al., 2007), have all been described previously. From our analyses, we identified zebrafish *vegfb*, which is syntenic to human VEGFB (not shown) and with orthologs that are present in other fish species. The placental growth factor (PGF) locus is duplicated in the zebrafish, fugu and stickleback. Zebrafish *pgfa* is syntenic with human PGF, and zebrafish *pgfb* is syntenic with *pgfa* (not shown), indicating that a fish-specific duplication event occurred during evolution.

To investigate the expression levels of all Vegf ligands and receptors, qPCR analyses were performed on embryos at 7.25 dpf (Fig. 1B). *vhl* mutants displayed a significant upregulation of *flt1* (2.42-fold), *kdr* (4.53-fold) and *kdr-like* (2.65-fold) receptors, accompanied by increased *vegfaa* (3.04-fold), *vegfab* (9.16-fold) and *vegfb* (2.70-fold) ligand expression. *flt4*, *vegfc*, *vegfd* and *pgfb* levels were not altered significantly, and *pgfa* could not be detected. These data suggest that Flt1-, Kdr- and Kdr-like-mediated signaling is increased in *vhl* mutants.

### *vhl* mutants display increased angiogenesis

We crossed *vhl* mutant alleles into a *kdr-like:egfp* transgenic (TG) background and observed a marked increase in the number of blood vessels throughout the *vhl*<sup>-/-</sup> embryo. Although vasculogenesis is seemingly unaffected at the morphological level (not shown), angiogenesis is enhanced, as first evidenced by the increase of cranial blood vessels at around 58 hours post-fertilization (hpf) (Fig. 2A). The trunk vasculature is unaffected at this stage; however, blood vessels appear dilated (Fig. 2B). At

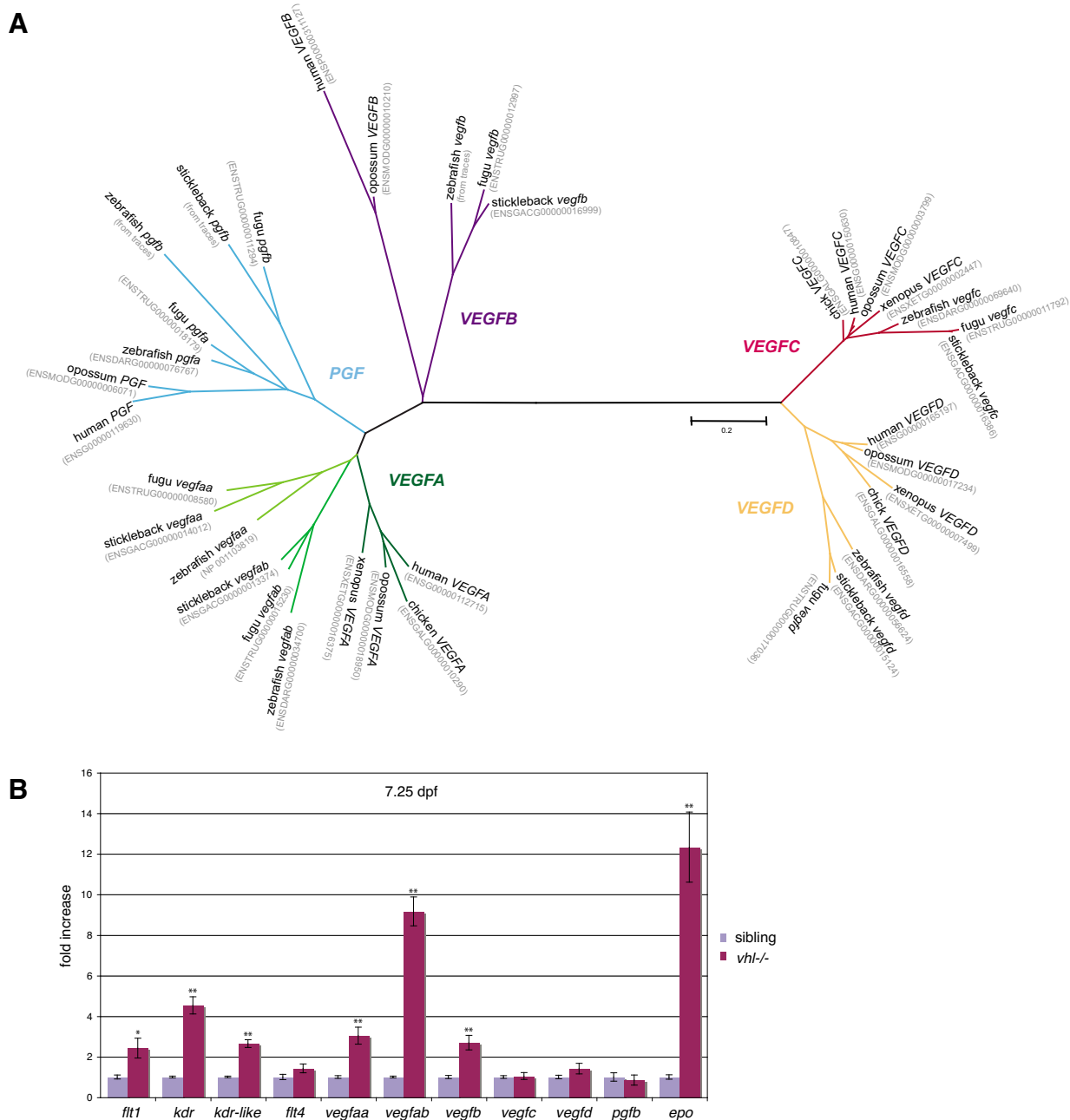


**Fig. 1. *vhl* mutants display increased Flt1, Kdr and Kdr-like signaling.** (A) Rooted neighbor-joining phylogenetic tree of vertebrate VEGF ligands. The different colors represent different classes of VEGF ligands. The bar indicates an evolutionary distance of 0.2 amino acid substitutions per position. (B) qPCR at 7.25 dpf revealed that, compared with siblings, the Vegf receptors *flt1*, *kdr* and *kdr-like*, and the Vegf ligands *vegfaa*, *vegfab* and *vegfb*, are significantly upregulated in *vhl* mutants. *erythropoietin* (*epo*) was used as a positive control. The threshold cycle (Ct) values were corrected for the *18S* housekeeping gene. *vhl* mutant cDNA concentrations were calculated in arbitrary units compared with the sibling average, and are represented as the fold change with the sibling value set to 1. A paired Student's *t*-test was used to determine significant expression differences. Error bars represent the standard error of the mean (s.e.m.). \**P*<0.05, \*\**P*<0.005.

3.5 dpf, blood vessels can be observed throughout the forebrain and midbrain of *vhl* mutants. Furthermore, compared with their siblings, most vessels in *vhl*<sup>-/-</sup> zebrafish appear dilated, including the ventral aorta (VA), branchial arches (AA), prosencephalic artery (PrA) and mesencephalic vein (MsV) (arrowheads, Fig. 2A IV). In the trunk, aberrant angiogenic sprouting emanates from

the intersomitic vessels (ISV), mainly in regions that are dorsal to the horizontal myoseptum (arrowheads, Fig. 2B XI). By 5.75 dpf, strong neovascularization of the entire *vhl*<sup>-/-</sup> brain is observed (Fig. 2A VI). Similarly, the trunk vasculature in *vhl* mutants is expanded, forming a complex of functional vessels (Fig. 2B XII) through which blood flow was observed (not shown).

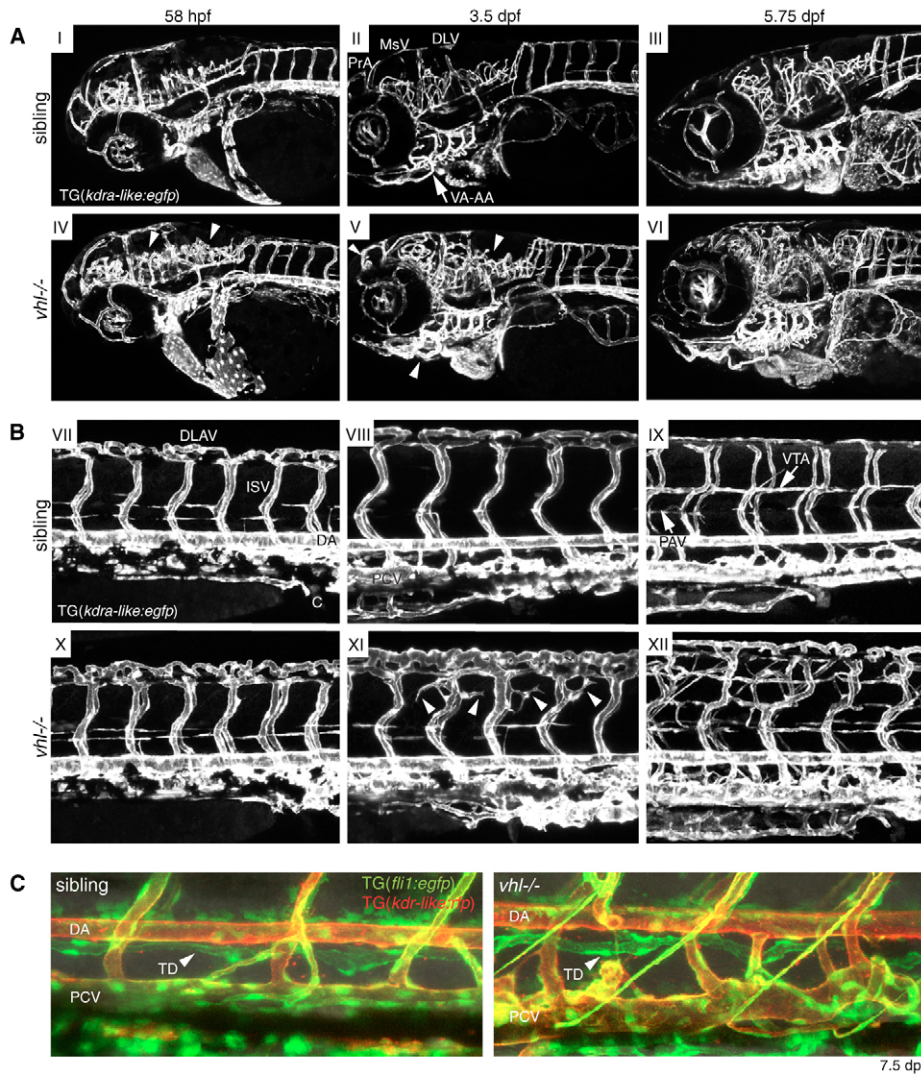


**Fig. 2. *vhl* mutants display increased angiogenesis.** (A) Confocal analysis of the cranial vasculature in *TG(kdr-like:egfp)* embryos. From 58 hpf, an increased number of cranial blood vessels are visible in the *vhl* mutant (arrowheads, panel IV). At 3.5 (V) and 5.75 dpf (VI), blood vessels are observed throughout the *vhl*<sup>-/-</sup> forebrain and midbrain. Compared with siblings (II), most *vhl*<sup>-/-</sup> vessels appear dilated, including the VA-AA, PrA and MsV (arrowheads, V). (B) Confocal analysis of the trunk vasculature in *TG(kdr-like:egfp)* embryos. At 58 hpf, no difference in vascular patterning is observed between *vhl* mutants (X) and their siblings (VII), although the *vhl*<sup>-/-</sup> DA, ISVs and DLAV appear dilated. At 3.5 dpf, aberrant angiogenic sprouts are observed in the *vhl* mutant (arrowheads, XI), which originate from the ISVs and are mainly located dorsal to the horizontal myoseptum. By 5.75 dpf, neovascularization of the *vhl*<sup>-/-</sup> trunk vasculature is observed (XII), forming a complex of functional vessels with blood flow (not shown). (C) Compared with age-matched siblings, lymphangiogenesis is unaffected in 7.5-dpf *vhl* mutants carrying the *flt1:egfp* (marking blood and lymph vessels) and *kdr-like:rfp* (marking blood vessels) transgenes. Arrowheads point to the TD just ventral to the DA. Anterior is to the left in all images. EGFP, enhanced green fluorescent protein; RFP, red fluorescent protein; PrA, prosencephalic artery; MsV, mesencephalic vein; DLV, dorsal longitudinal vein; VA-AA, ventral aorta-branchial arches; DLAV, dorsal longitudinal anastomotic vessel; ISV, intersegmental vessel; DA, dorsal aorta; PCV, posterior cardinal vein; C, cloaca; PAV, parachordal vessel; VTA, vertebral artery; TD, thoracic duct. Bars, 50  $\mu$ m.

To investigate whether lymphangiogenesis is affected, we examined 7.5-dpf *vhl* mutants expressing both the *flt1:egfp* (marking both blood and lymph vessels) and *kdr-like:rfp* (marking only blood vessels) transgenes. Although confocal analysis of the trunk revealed that *vhl* mutants display a slightly dilated thoracic duct (TD), lymphangiogenesis was not obviously affected (Fig. 2C). In accordance with our qPCR data showing unaltered *flt4*, *vegfc* and *vegfd* expression levels in *vhl* mutants, we conclude that the *vhl*<sup>-/-</sup> angiogenic response is restricted to the blood vasculature at the stages analyzed.

### Neovascularization, macular edema and retinal detachment in the *vhl*<sup>-/-</sup> retina

Since retinal vascular lesions are the most common and earliest manifestations of VHL disease (Wong et al., 2007), we investigated the *vhl* mutant eye vasculature. The zebrafish embryonic eye is nourished by choroidal vessels overlying the retinal pigmented epithelium (RPE) and by a central retinal artery, from which hyaloid vessels branch by angiogenesis and attach to the back of the lens (Alvarez et al., 2007). Confocal analysis of *vhl* mutant eyes

revealed a dramatic increase in both the choroidal (Fig. 3A I,III) and the hyaloid (Fig. 3A II,IV) vascular networks compared with siblings at 5.75 dpf.

VHL-associated retinal and CNS hemangioblastomas display increased expression of the chemokine receptor CXCR4 and its ligand SDF-1 in tumor and vascular cells (Zagzag et al., 2005). CXCR4 is regulated by HIF and VEGFA (Zagzag et al., 2006), and CXCR4/SDF-1 and VEGFA have been shown to synergize in the context of angiogenesis (Kryczek et al., 2005). In zebrafish, the *CXCR4* gene is duplicated into *cxc4a* and *cxc4b*, with both fulfilling distinct functions (Chong et al., 2001). In Fig. 3B, we show that *cxc4a* is expressed in blood vessels in the *vhl*<sup>-/-</sup> brain and retina, whereas in siblings, no vascular expression could be detected. *cxc4b* is expressed in the pronephric hematopoietic tissue (supplementary material Fig. S1), which is expanded in *vhl* mutants, as described previously (van Rooijen et al., 2009). Interestingly, although we see a marked increase in blood vessels throughout the *vhl* mutant embryo, *cxc4a*-positive blood vessels can only be observed in the distinct areas where high *vegfaa* mRNA expression is detected (supplementary material Fig. S1). This is most striking

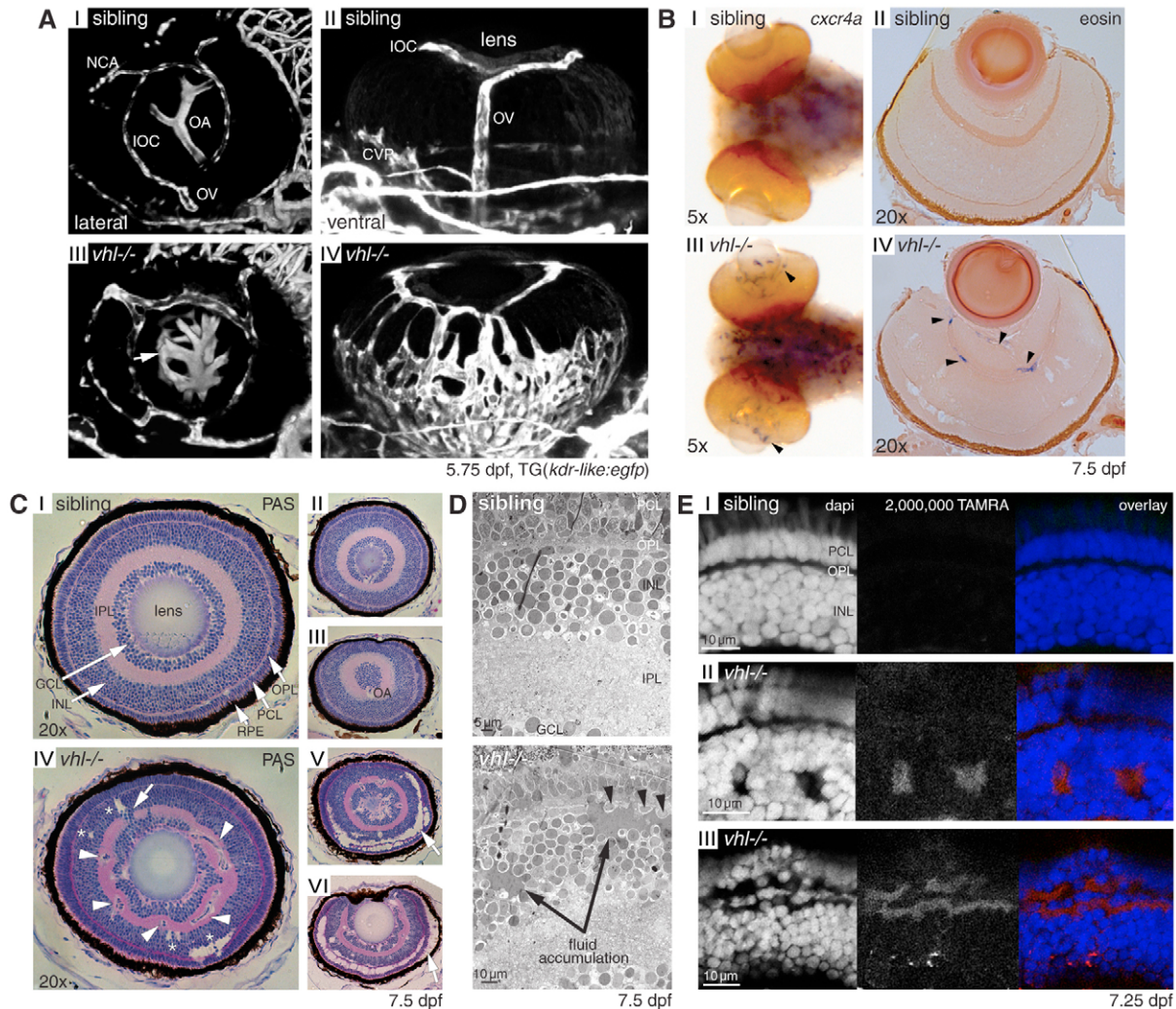


**Fig. 3. Neovascularization, macular edema and retinal detachments in the *vhl*<sup>-/-</sup> retina.** (A) Confocal analysis of the eye vasculature in TG(*kdr-like:egfp*) *vhl* mutant embryos reveals a dramatic increase in both the hyaloid (arrow, AIII, lateral view) and choroid (AIV, ventral view) vascular networks compared with siblings at 5.75 dpf. (B) In situ hybridization reveals *cxcr4a* expression in blood vessels (arrowheads) in the *vhl* mutant brain and retina, as shown in whole-mount (I,III) and eosin-counterstained (II,IV) sections through the eye. No vascular *cxcr4a* expression was detected at 7.5 dpf in siblings. (C) Histological analysis of periodic acid-Schiff (PAS)-stained sibling (I-III) and *vhl*<sup>-/-</sup> (IV-VI) retinas at 7.5 dpf. Although intraretinal vessels are not observed in the sibling eye, *vhl* mutant retinas revealed the presence of blood vessels (arrowheads, IV) that contain blood cells, predominantly in the IPL. Furthermore, several lesions were observed in the different retinal layers (asterisks, IV-VI), suggestive of macular edema predominantly in the INL and PCL. Retinal detachment of the retinal nerve layers from the RPE was also observed (arrow, VI). (D) Electron microscopy analysis of the *vhl*<sup>-/-</sup> retina at 7.5 dpf shows that these retinal lesions contain electron-dense material, confirming the development of macular edema. Fluid accumulation is observed between the nuclei of the INL, and reaching into the OPL and PCL. It even appears that nuclei from the INL are pushed out into the OPL (arrowheads) or the IPL (arrow, CIV). This was never observed in siblings. (E) Confocal analysis of sibling and *vhl* mutant retinas 20-25 hours after cardiac administration of 2,000,000 MW TAMRA at 7.25 dpf. Although retinal abnormalities were never observed in siblings (I), *vhl* mutants show TAMRA accumulation in the retinal lesions (II) and between the outer retinal cell layers (III). Bars, 5  $\mu$ m (D); 10  $\mu$ m (E). NCA, nasal ciliary artery; IOC, inner optic circle; OA, optic artery; OV, optic vein; CVP, choroidal vascular plexus; RPE, retinal pigmented epithelium; OPL, outer plexiform layer; IPL, inner plexiform layer; GCL, ganglion cell layer; INL, inner nuclear layer; PCL, photoreceptor layer.

in the *vhl*<sup>-/-</sup> brain and in the *vhl*<sup>-/-</sup> eye, where *cxcr4a*-positive blood vessels were detected in the retina and not in the neovascularized choroidal vessels overlying the RPE (Fig. 3B).

In mammals, primary retinal vessels branch to form intraretinal capillaries that form plexi within the inner and outer plexiform layers; by contrast, these networks of vessels are not present in the largely avascular zebrafish eye (Wittenberg and Wittenberg, 1974; Alvarez et al., 2007; Fruttiger, 2007). Accordingly, intraretinal

vessels are not observed in the sibling eye at 7.5 dpf (Fig. 3B,C I-III). Histological analysis of the *vhl*<sup>-/-</sup> retina, however, reveals the presence of *cxcr4a*-positive blood vessels (containing blood cells), predominantly in the inner plexiform layer (IPL) at 7.5 dpf (arrowheads, Fig. 3B,C IV).

A common clinical feature of VHL-associated and diabetic retinopathies is the development of macular edema, which is the accumulation of fluid in the central part of the retina (Tranos et

al., 2004). Although a broad range of pathologies can induce macular edema, in these particular instances, edema is caused by fluid leakage from the neovascularized retinal capillaries (breakage of the inner retina-blood barrier) (Tranos et al., 2004). Owing to the hydrostatic characteristics of the distinct retinal nerve layers (with the plexiform layers being high-resistance barriers to flow) (Antcliff et al., 2001), macular edema is mainly observed in the outer retinal nerve layers, including the inner nuclear layer (INL) and the photoreceptor cell layer (PCL) (Ciulla et al., 2003; Tranos et al., 2004). If left untreated, it can cause detachment of the retinal layers from the RPE and lead to vision loss.

Histological analyses revealed multiple retinal lesions in the outer retinal layers of the *vhl*<sup>-/-</sup> eye (asterisks, Fig. 3C IV-VI), suggestive of macular edema. This was most pronounced in the ventral half of the mutant eye. In 95.8% ( $n=23/24$ ) of the examined *vhl*<sup>-/-</sup> eyes, severe macular edema was observed predominantly in the INL and PCL (Fig. 3C IV-VI), and mostly in close proximity to the outer plexiform layer (OPL). In 14.3% ( $n=4/28$ ) of the *vhl*<sup>-/-</sup> eyes, additional sites of retinal detachment of the retinal nerve layers from the RPE were observed (Fig. 3C VI). These retinal abnormalities were never observed in age-matched sibling eyes ( $n=24/24$ ). Electron microscopy analysis confirmed these *vhl*<sup>-/-</sup> retinal lesions to represent macular edema since they contained electron-dense material that was not observed in siblings ( $n=2/2$ ) at 7.5 dpf. As shown in Fig. 3D, accumulation of this material was observed between the nuclei of the INL, and reaching into the OPL and PCL. It even appeared that nuclei from the INL were pushed out into the OPL (arrowheads, Fig. 3D) or IPL (white arrow, Fig. 3C IV) by the accumulating fluid.

To investigate whether the observed macular edema is caused by vascular leakage, we performed fluorescent angiographies at 6 dpf with a high molecular weight rhodamine-dextran conjugate (2,000,000 MW TAMRA) that is normally too large to pass through the vessel wall. At approximately 20-25 hours post-injection, embryos were fixed and subjected to confocal analysis. In Fig. 3E, nuclear counterstaining revealed that while retinal abnormalities were never observed in siblings, TAMRA clearly accumulates in the *vhl*<sup>-/-</sup> retinal lesions and at distinct locations between the outer retinal cell layers, indicating sites of macular edema.

### The *vhl*<sup>-/-</sup> retinal vasculature is leaky

Confocal analysis of the optic artery and the inner optic circle after TAMRA injection in 6-dpf *kdr-like:egfp* transgenic embryos revealed severe vascular leakage through the vessel wall into the surrounding tissue (white arrows) in *vhl* mutants. Three-dimensional (3D) reconstructions from confocal stacks are presented in Fig. 4A-C (see supplementary material Movie 1 for a 3D movie animation of these images). Taken together, these data suggest that neovascularization of the choroidal vasculature in the *vhl*<sup>-/-</sup> eye induces vascular leakage, leading to severe macular edema in the outer layers of the retina, irregularities in the retinal layers, and eventually retinal detachment. Although *vhl* mutant embryos do not develop typical hemangioblastomas, these data indicate that the *vhl*<sup>-/-</sup>-associated angiogenic phenotype shares distinct characteristics with VHL-disease manifestations, and more generally with other vascular retinopathies.

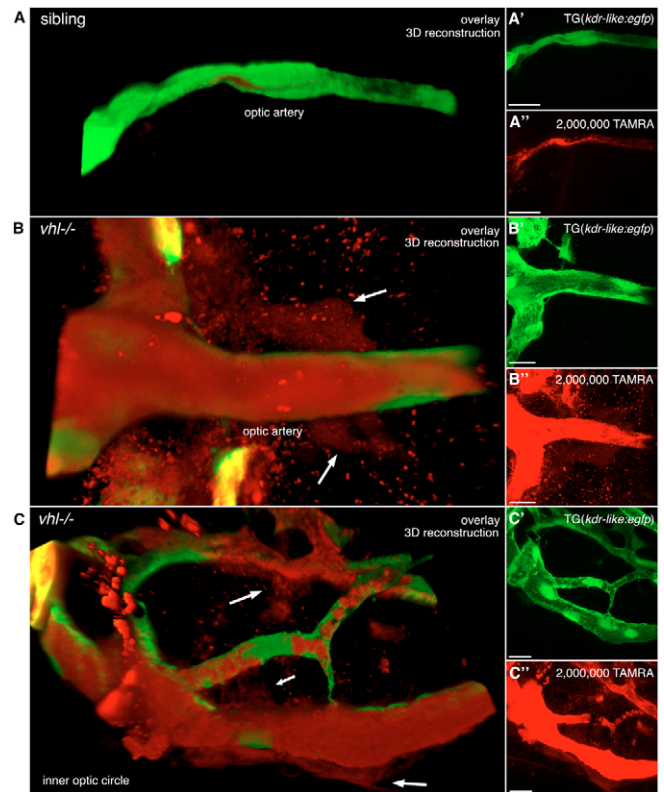


**Fig. 4. The *vhl*<sup>-/-</sup> retinal vasculature is leaky.** Confocal analysis of the retinal vasculature 20-25 hours after TAMRA injection in 7-dpf TG(*kdr-like:egfp*) embryos. (A) A 3D reconstruction of the sibling optic artery revealed that TAMRA was contained within the blood vessel. (B,C) *vhl* mutants display severe vascular leakage through the vessel wall into the surrounding tissue (arrows), as shown in the optic artery (B) and the inner optic circle (C). (A'-C'') Z-stack projections for *kdr-like:egfp*; (A''-C'') Z-stack projections for TAMRA. Bars, 10  $\mu$ m.

### Vegf receptor tyrosine kinase inhibition blocks *vhl*<sup>-/-</sup> pathological angiogenesis

To investigate whether the VEGF signaling pathway is necessary and sufficient to induce the observed *vhl*-associated neovascularization in our mutant zebrafish, we treated embryos with two multi-targeted VEGF receptor tyrosine kinase inhibitors: 676475 (Calbiochem) and sunitinib malate (or Sutent). Blocking VEGF has been shown to inhibit vasculogenesis, angiogenic formation of the ISVs, and formation of the DLAV, when administered very early during zebrafish development (Chan et al., 2002; Lee et al., 2002). Therefore, to ensure proper patterning of the cranial and trunk vasculature prior to treatment, we initiated exposure to each individual VEGFR inhibitor at 58 hpf, when the first vascular abnormalities were observed in *vhl* mutants. Embryos were incubated with 10  $\mu$ M 676475, 0.2  $\mu$ M sunitinib or DMSO (vessel control) in embryo medium for 3 days (Fig. 5). Confocal analysis of the head, eye and trunk vasculature at 5.75 dpf revealed that the pathological angiogenesis in *vhl* mutants was almost completely blocked by 676475, and completely blocked by sunitinib treatment. Unfortunately, owing to the accumulation and autofluorescence of the yellow substance from the sunitinib solution in the skin (which also occurs in human patients), it was not possible

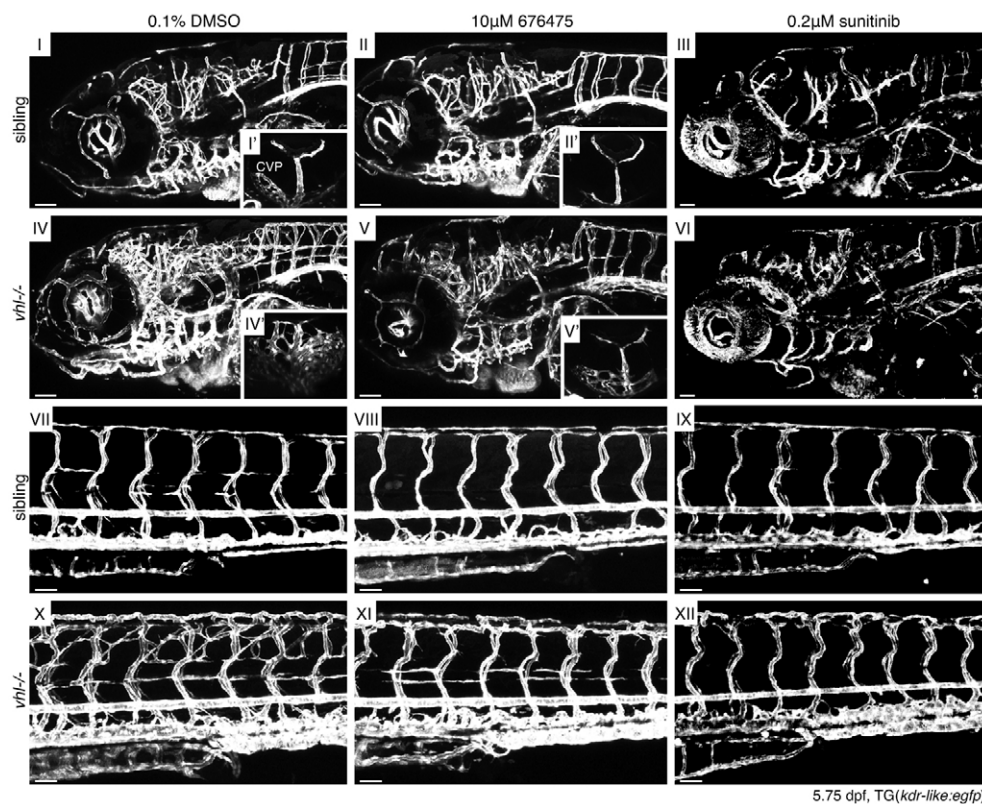


**Fig. 5. Vegf receptor tyrosine kinase inhibition blocks *vhl*<sup>-/-</sup> pathological angiogenesis.** TG(*kdr-like:egfp*) embryos were incubated in embryo medium containing 0.1% DMSO (vessel control), 10 μM FLT1/KDR tyrosine kinase inhibitor 676475 (Calbiochem) or 0.2 μM sunitinib at 58 hpf. Confocal analysis of the head (I–VI), eye (inserts, ventral view) and trunk (VII–XII) vasculature at 5.75 dpf revealed that the formation of new vessels in *vhl* mutants is blocked by 676475 and – even more dramatically – by sunitinib. CVP, choroid vascular plexus. Bars, 50 μm.

to analyze the choroidal vasculature by confocal microscopy. Our results indicate that *vhl* mutants provide a new and clinically relevant model that is suitable for large-scale compound screens for anti-angiogenic agents and combinatorial treatments.

## DISCUSSION

VHL disease is characterized by the development of highly vascularized neoplasms that overexpress a variety of angiogenic factors, including VEGFA, KDR and CXCR4 (Chan et al., 2005; Zagzag et al., 2005; Liang et al., 2007; Park et al., 2007). Similarly, we show that loss of *vhl* in zebrafish embryos induces severe pathological neovascularization, with increased Vegf signaling and *cxcr4a* expression in the brain and retina. Comparable to VHL-associated retinal neoplasms, diabetic retinopathy and age-related macular degeneration, we show by TAMRA angiographies that vascular abnormalities in the *vhl*<sup>-/-</sup> retina lead to vascular leakage, severe macular edema and retinal detachment.

Although hemangioblastomas were not found in our *vhl* mutant embryos or in heterozygote adult zebrafish, the observed *vhl*<sup>-/-</sup> retinal neovascularization appears to be more similar to a new class of ocular VHL disease that was more recently identified in a large prospective case study (Chew, 2005). Of the VHL patients with ocular lesions, a novel ocular manifestation similar to diabetic retinal neovascularization was identified in 17 patients (8.3%). Although these neovascular lesions are less common than hemangioblastomas, the actual incidence might be higher owing to the fact that they have not been attributed to loss of pVHL.

Vascular abnormalities have been observed in murine *Vhlh* (also known as *Vhl*) models. Conventional *Vhlh* knockout mice (Gnarra et al., 1997), and mice harboring a targeted deletion of *Vhlh* in

endothelial cells (Tang et al., 2006), are embryonic lethal [death occurs between embryonic day (E)9.5–12.5] owing to hemorrhagic lesions and vascular abnormalities in the placenta. Deletion of *Vhlh* in the epidermis (Boutin et al., 2008) and liver (Haase et al., 2001; Rankin et al., 2005) resulted in increased angiogenesis in the targeted organ systems, and mosaic *Vhlh* inactivation (Ma et al., 2003) or systemic *Vhlh*<sup>+/-</sup> mice often develop hepatic cavernous hemangiomas. However, hemangioblastomas of the retina and CNS have not been found in any *Vhlh* mouse model. Therefore, the fact that the *vhl* zebrafish survives past embryogenesis, and that additional organ systems are affected, underscores the complementary nature of these two models in studying hypoxia-induced angiogenesis.

It was shown that the development of vascularized tumors in *Vhlh*-deficient livers was entirely dependent on HIF (Rankin et al., 2005). This finding supports our data, indicating that systemic stabilization of Hif through the loss of *vhl* is the most likely initiator of *vegf*-induced *vhl*<sup>-/-</sup> neovascularization. However, it has been shown that, during mouse development, endothelial cells require *Vhlh* for correct vascular patterning and maintenance of vascular integrity (Tang et al., 2006), through HIF-independent regulation of fibronectin deposition (Ohh et al., 1998; Tang et al., 2006). Therefore VHL-induced changes in the extravascular matrix probably contribute to the characteristics of the vascular neoplasms in VHL patients, however, this needs to be investigated further.

In recent years, VEGF, its receptors and the HIF signaling pathway have, in general, received considerable attention as potential therapeutic targets for cancer and other angiogenesis-related disorders. However, the current in vitro and in vivo models for angiogenesis fail, to a certain extent, to recapitulate the

complexity of angiogenesis and its microenvironment, or to allow in vivo functional evaluations (Taraboletti and Giavazzi, 2004). Recently, an adult zebrafish model for hypoxia-induced retinal angiogenesis was presented (Cao et al., 2008). Adult zebrafish that were exposed to 10% air-saturated water developed severe retinal neovascularization after 3-12 days of incubation. The anti-VEGF agents sunitinib and ZM323881 effectively blocked hypoxia-induced neovascularization, demonstrating the clinical relevancy of this retinal angiogenesis model. However, these studies are invasive and an adult zebrafish system is less suitable for high-throughput and cost-effective screening of novel compounds owing to the minimal water volume required.

In this study, we showed that *vhl*<sup>-/-</sup> embryos develop severe neovascularization of the choroid and hyaloid vessels; this was blocked by treatment with the tyrosine kinase inhibitors 676475 and sunitinib. In diabetic retinopathy, age-related macular degeneration, and VHL-associated retinal neoplasms, the prominent vascular abnormalities induce vascular leakage, macular edema and retinal detachment, which can lead to a complete loss of vision (Arjamaa and Nikinmaa, 2006). Similarly, we also observed severe macular edema and retinal detachment in *vhl* mutants, which was not described in the adult zebrafish retinal angiogenesis model (Cao et al., 2008).

Additionally, we observed an early and fully penetrant increased angiogenic response throughout the *vhl*<sup>-/-</sup> embryo. Wild-type zebrafish embryos that were kept under hypoxic conditions (partial pressure of oxygen of 8.7 kPa) from 1 to 15 dpf did not show significant changes in vascularization, or in the basic pattern of the vascular bed of the trunk and gut, as compared with normoxic animals, and the perfusion rate was increased in the trunk musculature, unchanged in the brain and reduced in the gut (Schwerte et al., 2003). Since, at lower oxygen levels, zebrafish embryos do not develop properly (Schwerte et al., 2003) and adult zebrafish die (Cao et al., 2008), the induced hypoxia in these studies might not have been low enough to induce a similar angiogenic response as in *vhl*<sup>-/-</sup> embryos.

Therefore, our data indicate that *vhl* mutant zebrafish embryos represent a unique and clinically relevant angiogenesis model where, in the context of systemic hypoxia signaling, the process of pathological angiogenesis and vascular retinopathies can be studied non-invasively in a tissue-specific context under normoxic conditions. Using a blood vessel-specific transgenic background, *vhl* mutant embryos allow for a cost-effective and efficient way to screen pharmacological agents for anti-angiogenic properties and combinatorial treatments in a whole organism setting.

## METHODS

### Zebrafish lines

Zebrafish were maintained as described previously (Westerfield, 1995). Animal experiments were conducted in accordance with the Dutch guidelines for the care and use of laboratory animals, with the approval of the Animal Experimentation Committee (DEC) of the Royal Netherlands Academy of Arts and Sciences (KNAW). The mutant alleles *vhl*<sup>hu2117</sup>(Q23X) and *vhl*<sup>hu2081</sup>(C31X) (van Rooijen et al., 2009) were out-crossed to the transgenic lines TG(*kdr-like:egfp*)<sup>s843</sup> (Jin et al., 2005), TG(*fli1a:egfp*)<sup>y1</sup> (Lawson and Weinstein, 2002) and TG(*kdr-like:ras-cherry*)<sup>s916</sup> (Chi et al., 2008; Hogan et al., 2009). Unless indicated otherwise, transheterozygote

embryos (*vhl*<sup>hu2117</sup>/*vhl*<sup>hu2081</sup>) were used in experimental assays. Where indicated, embryos were anesthetized with MS222 (final concentration of 0.17 mg/ml).

### Phylogenetic analysis

Phylogenetic analysis of the zebrafish Vegf ligands was performed with the MEGA3 software package (Kumar et al., 2004), using the PDGF and VEGF family domain (cd00135) from NCBI's Conserved Domain Database (CDD). Amino acid sequences were aligned with ClustalW and a phylogenetic tree was constructed using a neighbor-joining algorithm. The resulting tree was tested using 1000 bootstrap resamplings. Pairwise distances were calculated with the PAM substitution matrix. Identification of vertebrate VEGF ligands and synteny analysis was performed using the Ensembl database (<http://www.ensembl.org>), release 44, April 2007. Sequences are available upon request.

### Quantitative real-time PCR

For total RNA isolation, a maximum of 40 *vhl* mutants and siblings per clutch were homogenized by shredding in 600 µl of RTL lysis buffer (Qiagen RNeasy kit) containing 10% beta-mercaptoethanol. One volume of 70% ethanol was added and the homogenate was loaded onto a column for total RNA isolation according to the manufacturer's protocol, followed by DNaseI (Promega) treatment. The RNA quality and concentration were determined using a NanoDrop, and verified by gel electrophoresis. cDNA was synthesized from total RNA (1-5 µg) with random hexamers (Biolegio, [www.biolegio.nl](http://www.biolegio.nl)) using reverse transcriptase M-MLV (Promega). Primer sets were designed using Primer3 (<http://frodo.wi.mit.edu/>) and Limstall (<http://limstall.niob.knaw.nl/>) software, with an optimal product size of 150-200 base pairs that, where possible, spanned two exons to avoid genomic contamination. The PCR efficiency and optimal melting temperatures were determined per primer set, and the specificity was verified by gel electrophoresis using standard real-time PCR on zebrafish cDNA. See supplementary material Table S1 for primer sequences and melting temperatures. qPCR was performed using the MyIQ single color real-time PCR detection system and software (Bio-Rad). Each reaction contained: 12.5 µl SYBR Green fluorescent label (Bio-Rad), 3 µl of 1.5 µM primer mix, 4.5 µl MQ and 5 µl cDNA (10ng/µl). Cycling conditions were: 95°C for 3 minutes; 40 cycles of 95°C for 10 seconds and the optimal primer temperature for 45 seconds; followed by 95°C for 1 minute; and finally 65°C for 1 minute. All reactions were performed in triplicate on cDNA isolated from at least two different clutches of pooled *vhl* mutants and siblings. Ct values were corrected for the 18S housekeeping gene (Cooper et al., 2006). *vhl* mutant cDNA concentrations were calculated in arbitrary units compared with the sibling average, and are represented as the fold change with the sibling value set to 1. A paired Student's *t*-test was used to determine significant differences in expression between *vhl* mutants and siblings.

### Confocal analysis of blood vessels

Anesthetized embryos were embedded in 0.5% agarose on a coverslip, and confocal images were collected on a Leica DM IRE2 microscope (Leica Microsystems) using 10×, 20×, 40× and 63× objectives. 3D reconstructions of confocal stacks were generated using the Volocity software package (Improvision, [www.improvision.com](http://www.improvision.com)).

## TRANSLATIONAL IMPACT

### Clinical issue

von Hippel-Lindau disease (VHL) is a rare, genetic multisystem disorder characterized by the abnormal growth of blood vessels and tumors. Between 60% and 80% of all patients have benign hemangioblastomas of the retina and central nervous system (CNS) that frequently cause neurological morbidity and mortality. VHL patients can also develop retinal neovascularization (also termed angiogenesis; the formation of new blood vessels), similar to diabetic retinopathy and age-related macular degeneration. Angiogenic retinopathies exhibit vascular leakage, macular edema (fluid accumulation) and detachment of the retina, and are the biggest cause of blindness in the Western world, with very limited treatment options. Unfortunately, the current models for angiogenesis do not fully recapitulate the complexity of angiogenic-related disorders. For instance, hemangioblastomas of the retina and CNS have not been found in any of the VHL mouse models.

The VHL tumor suppressor gene, *VHL*, is crucial for oxygen homeostasis. Its loss causes upregulation of HIF (hypoxia-inducible factor), a transcription factor with a central role in oxygen-regulated gene expression, which in turn increases the expression of hypoxia-inducible mRNAs, including those encoding vascular endothelial growth factor A (VEGFA), VEGFA receptors, and proteins involved in the HIF signaling pathway

### Results

In this study, the authors show that zebrafish *vhl* mutants provide an in vivo model for pathological angiogenesis and vascular retinopathies. Using blood vessel-specific transgenes, they show that *vhl* mutants develop severe neovascularization in the brain, eye and trunk. The retinal vasculature of *vhl*<sup>-/-</sup> zebrafish is leaky, with severe macular edema and retinal detachment, mimicking human angiogenic retinopathies. As in humans, the zebrafish VEGFA orthologs, *Vegfaa/Vegfab* and *Vegfb*, are upregulated by loss of *vhl*, and are key effectors of the *vhl*<sup>-/-</sup> angiogenic phenotype; treatment with VEGF receptor inhibitors can block pathological angiogenesis in mutant fish.

### Implications and future directions

These zebrafish *vhl* mutants can be used to understand the mechanisms underlying the development of vascular lesions in VHL disease, and are a unique and clinically relevant angiogenesis model, as pathological angiogenesis and vascular retinopathies can be studied non-invasively under normoxic conditions. Zebrafish *vhl* mutant embryos with fluorescently-labeled blood vessels are also a cost-effective and efficient model for whole organism screening of anti-angiogenic pharmacological agents and combinatorial therapies.

doi:10.1242/dmm.005306

### Histology

Transversal plastic sections (7 μm) were stained with periodic acid-Schiff (PAS) or eosin using standard protocols.

### Fluorescent dye injections

Anesthetized embryos were embedded in 0.5% agarose and were administered with 10 mg/ml of 2,000,000 MW tetramethyl rhodamine (TAMRA; Molecular Probes) by cardiac injection at 6 dpf. Only embryos exhibiting TAMRA throughout the cardiovascular system immediately after injection were analyzed further. At approximately 20-25 hours post-injection, embryos were fixed with 4% PFA for 2 hours at room temperature or overnight at 4°C. Retinal vascular leakage was determined by confocal analyses on sections cut on either a Microm HM650V (<http://www.microm-online.com>) vibratome (75-100 μm) or a Leica CM3050 cryostat (50 μm).

### In situ hybridization

Whole-mount in situ hybridization was performed as described (Schulte-Merker, 2002) with minor modifications. Antisense digoxigenin (Roche)-labeled mRNA probes for *cxcra4a* (Chong et al., 2001), *cxcra4b* (Chong et al., 2001) and *vegfaa* (Liang et al., 2001) were generated as described, and purified using NucleoSpin RNA clean-up columns (Machery-Nagel, [www.machery-nagel.com](http://www.machery-nagel.com)). To improve probe penetration, 7.5-day-old larvae were partially cut open at the level of the yolk sac extension after proteinase K permeabilization. After in situ hybridization, pigmented embryos were bleached in a solution containing 0.5× SSC, 5% formamide and 10% H<sub>2</sub>O<sub>2</sub> for 20-40 minutes. Embryos were mounted in 2% methylcellulose on a depression slide and imaged on a Zeiss axioplan microscope with a 5× objective.

### Transmission electron microscopy

Embryos were fixed in Karnovsky fixative (2% paraformaldehyde, 2.5% glutaraldehyde, 0.08 M Na cacodylate, pH 7.4, 0.25 mM calcium chloride, 0.5 mM magnesium chloride, set to pH 7.4) for at least 24 hours at 4°C. Samples were postfixed in 1% osmium tetroxide and embedded in Epon 812. Ultra-thin sections (60 nm) were contrasted with 3% uranyl magnesium acetate and lead citrate, and viewed with a Jeol JEM 1010 transmission electron microscope.

### VEGF receptor tyrosine kinase inhibitor treatments

2.5-day-old embryos were treated with 10 μM of the VEGF receptor tyrosine kinase inhibitor 676475 (Calbiochem, <http://www.merckbiosciences.co.uk/>; single dose) or 0.2 μM of sunitinib malate (Selleck Chemicals, [www.selleckchem.com](http://www.selleckchem.com); daily refreshment) in embryo medium (Westerfield, 1995), at 28°C, in 6-well culture plates containing 30 embryos per well. Control embryos were incubated with an equivalent amount of DMSO solution under the same conditions. Experiments were performed in triplicate.

### ACKNOWLEDGEMENTS

This project was funded by the Dutch Cancer Society (UU-2006-3565). R.H.G. is supported by a VIDJ award (NWO). F.J.v.E. is supported by Cancer Research UK (C23207/A8066), and J.B. by the Stichting Vrienden van het Hubrecht. We gratefully acknowledge Bart Weijts (Veterinary Medicine, Utrecht University) for help with quantitative real-time PCR; Roel Goldschmeding and Kevin van de Ven (Department of Pathology, UMC Utrecht) for transmission electron microscopy; Henk Verheul and Kristy Gotink (Department of Medical Oncology, VUMC Amsterdam) for helpful discussions; and Lasse Dahl Jensen (Karolinska Institute, Sweden) for sharing information on sunitinib treatments in zebrafish.

### COMPETING INTERESTS

The authors declare no competing financial interests.

### AUTHOR CONTRIBUTIONS

E.v.R., I.L., J.B. and J.K. performed the experiments; E.v.R., E.E.V., F.J.v.E., R.H.G. and S.S.-M. designed the research, analyzed data, and checked or improved the manuscript; E.v.R. drafted the manuscript.

### SUPPLEMENTARY MATERIAL

Supplementary material for this article is available at <http://dmm.biologists.org/lookup/suppl/doi:10.1242/dmm.004036/-/DC1>

Received 21 July 2009; Accepted 21 November 2009.

### REFERENCES

Alvarez, Y., Cederlund, M. L., Cottell, D. C., Bill, B. R., Ekker, S. C., Torres-Vazquez, J., Weinstein, B. M., Hyde, D. R., Vihtelic, T. S. and Kennedy, B. N. (2007). Genetic determinants of hyaloid and retinal vasculature in zebrafish. *BMC Dev. Biol.* **7**, 114.

- Antcliff, R. J., Hussain, A. A. and Marshall, J.** (2001). Hydraulic conductivity of fixed retinal tissue after sequential excimer laser ablation: barriers limiting fluid distribution and implications for cystoid macular edema. *Arch. Ophthalmol.* **119**, 539-544.
- Arjamaa, O. and Nikinmaa, M.** (2006). Oxygen-dependent diseases in the retina: role of hypoxia-inducible factors. *Exp. Eye Res.* **83**, 473-483.
- Bahary, N., Goishi, K., Stuckenzholz, C., Weber, G., Leblanc, J., Schafer, C. A., Berman, S. S., Klagsbrun, M. and Zon, L. I.** (2007). Duplicate VegfA genes and orthologues of the KDR receptor tyrosine kinase family mediate vascular development in the zebrafish. *Blood* **110**, 3627-3636.
- Bluyssen, H. A., Lolkema, M. P., van Beest, M., Boone, M., Snijckers, C. M., Los, M., Gebbink, M. F., Braam, B., Holstege, F. C., Giles, R. H. et al.** (2004). Fibronectin is a hypoxia-independent target of the tumor suppressor VHL. *FEBS Lett.* **556**, 137-142.
- Boutin, A. T., Weidemann, A., Fu, Z., Mesropian, L., Gradin, K., Jamora, C., Wiesener, M., Eckardt, K. U., Koch, C. J., Ellies, L. G. et al.** (2008). Epidermal sensing of oxygen is essential for systemic hypoxic response. *Cell* **133**, 223-234.
- Bussmann, J., Bakkers, J. and Schulte-Merker, S.** (2007). Early endocardial morphogenesis requires *Scl/Tal1*. *PLoS Genet.* **3**, e140.
- Bussmann, J., Lawson, N., Zon, L. and Schulte-Merker, S.** (2008). Zebrafish VEGF receptors: a guideline to nomenclature. *PLoS Genet.* **4**, e1000064.
- Cao, R., Jensen, L. D., Soll, I., Hauptmann, G. and Cao, Y.** (2008). Hypoxia-induced retinal angiogenesis in zebrafish as a model to study retinopathy. *PLoS ONE* **3**, e2748.
- Carmeliet, P.** (2000). Mechanisms of angiogenesis and arteriogenesis. *Nat. Med.* **6**, 389-395.
- Carmeliet, P.** (2005). VEGF as a key mediator of angiogenesis in cancer. *Oncology* **69 Suppl. 3**, 4-10.
- Chan, C. C., Chew, E. Y., Shen, D., Hackett, J. and Zhuang, Z.** (2005). Expression of stem cells markers in ocular hemangioblastoma associated with von Hippel-Lindau (VHL) disease. *Mol. Vis.* **11**, 697-704.
- Chan, J., Bayliss, P. E., Wood, J. M. and Roberts, T. M.** (2002). Dissection of angiogenic signaling in zebrafish using a chemical genetic approach. *Cancer Cell* **1**, 257-267.
- Chew, E. Y.** (2005). Ocular manifestations of von Hippel-Lindau disease: clinical and genetic investigations. *Trans. Am. Ophthalmol. Soc.* **103**, 495-511.
- Chi, N. C., Shaw, R. M., De Val, S., Kang, G., Jan, L. Y., Black, B. L. and Stainier, D. Y.** (2008). Foxn4 directly regulates *tbx2b* expression and atrioventricular canal formation. *Genes Dev.* **22**, 734-739.
- Chong, S. W., Emelyanov, A., Gong, Z. and Korzh, V.** (2001). Expression pattern of two zebrafish genes, *cxcr4a* and *cxcr4b*. *Mech. Dev.* **109**, 347-354.
- Ciulla, L. A., Amador, A. G. and Zinman, B.** (2003). Diabetic retinopathy and diabetic macular edema: pathophysiology, screening, and novel therapies. *Diabetes Care* **26**, 2653-2664.
- Cooper, C. A., Handy, R. D. and Bury, N. R.** (2006). The effects of dietary iron concentration on gastrointestinal and branchial assimilation of both iron and cadmium in zebrafish (*Danio rerio*). *Aqua. Toxicol.* **79**, 167-175.
- Covassin, L. D., Villefranc, J. A., Kaceris, M. C., Weinstein, B. M. and Lawson, N. D.** (2006). Distinct genetic interactions between multiple Vegf receptors are required for development of different blood vessel types in zebrafish. *Proc. Natl. Acad. Sci. USA* **103**, 6554-6559.
- Dewhirst, M. W., Cao, Y. and Moeller, B.** (2008). Cycling hypoxia and free radicals regulate angiogenesis and radiotherapy response. *Nat. Rev. Cancer* **8**, 425-437.
- Forsythe, J. A., Jiang, B. H., Iyer, N. V., Agani, F., Leung, S. W., Koos, R. D. and Semenza, G. L.** (1996). Activation of vascular endothelial growth factor gene transcription by hypoxia-inducible factor 1. *Mol. Cell. Biol.* **16**, 4604-4613.
- Fruittiger, M.** (2007). Development of the retinal vasculature. *Angiogenesis* **10**, 77-88.
- Gleadle, J. M., Ebert, B. L., Firth, J. D. and Ratcliffe, P. J.** (1995). Regulation of angiogenic growth factor expression by hypoxia, transition metals, and chelating agents. *Am. J. Physiol.* **268**, C1362-C1368.
- Gnarra, J. R., Ward, J. M., Porter, F. D., Wagner, J. R., Devor, D. E., Grinberg, A., Emmert-Buck, M. R., Westphal, H., Klausner, R. D. and Linehan, W. M.** (1997). Defective placental vasculogenesis causes embryonic lethality in VHL-deficient mice. *Proc. Natl. Acad. Sci. USA* **94**, 9102-9107.
- Haase, V. H., Glickman, J. N., Socolovsky, M. and Jaenisch, R.** (2001). Vascular tumors in livers with targeted inactivation of the von Hippel-Lindau tumor suppressor. *Proc. Natl. Acad. Sci. USA* **98**, 1583-1588.
- Hogan, B. M., Bos, F. L., Bussmann, J., Witte, M., Chi, N. C., Duckers, H. J. and Schulte-Merker, S.** (2009). *Ccbe1* is required for embryonic lymphangiogenesis and venous sprouting. *Nat. Genet.* **41**, 396-398.
- Isogai, S., Horiguchi, M. and Weinstein, B. M.** (2001). The vascular anatomy of the developing zebrafish: an atlas of embryonic and early larval development. *Dev. Biol.* **230**, 278-301.
- Jin, S. W., Beis, D., Mitchell, T., Chen, J. N. and Stainier, D. Y.** (2005). Cellular and molecular analyses of vascular tube and lumen formation in zebrafish. *Development* **132**, 5199-5209.
- Kaelin, W. G.** (2005). Proline hydroxylation and gene expression. *Annu. Rev. Biochem.* **74**, 115-128.
- Kietzmann, T., Roth, U. and Jungermann, K.** (1999). Induction of the plasminogen activator inhibitor-1 gene expression by mild hypoxia via a hypoxia response element binding the hypoxia-inducible factor-1 in rat hepatocytes. *Blood* **94**, 4177-4185.
- Kryczek, I., Lange, A., Mottram, P., Alvarez, X., Cheng, P., Hogan, M., Moons, L., Wei, S., Zou, L., Machelon, V. et al.** (2005). CXCL12 and vascular endothelial growth factor synergistically induce neoangiogenesis in human ovarian cancers. *Cancer Res.* **65**, 465-472.
- Kumar, S., Tamura, K. and Nei, M.** (2004). MEGA3: Integrated software for Molecular Evolutionary Genetics Analysis and sequence alignment. *Brief. Bioinform.* **5**, 150-163.
- Lawson, N. D. and Weinstein, B. M.** (2002). In vivo imaging of embryonic vascular development using transgenic zebrafish. *Dev. Biol.* **248**, 307-318.
- Lee, P., Goishi, K., Davidson, A. J., Mannix, R., Zon, L. and Klagsbrun, M.** (2002). Neupilin-1 is required for vascular development and is a mediator of VEGF-dependent angiogenesis in zebrafish. *Proc. Natl. Acad. Sci. USA* **99**, 10470-10475.
- Lee, S., Chen, T. T., Barber, C. L., Jordan, M. C., Murdock, J., Desai, S., Ferrara, N., Nagy, A., Roos, K. P. and Iruela-Arispe, M. L.** (2007). Autocrine VEGF signaling is required for vascular homeostasis. *Cell* **130**, 691-703.
- Liang, D., Chang, J. R., Chin, A. J., Smith, A., Kelly, C., Weinberg, E. S. and Ge, R.** (2001). The role of vascular endothelial growth factor (VEGF) in vasculogenesis, angiogenesis, and hematopoiesis in zebrafish development. *Mech. Dev.* **108**, 29-43.
- Liang, X., Shen, D., Huang, Y., Yin, C., Bojanowski, C. M., Zhuang, Z. and Chan, C. C.** (2007). Molecular pathology and CXCR4 expression in surgically excised retinal hemangioblastomas associated with von Hippel-Lindau disease. *Ophthalmology* **114**, 147-156.
- Liao, D. and Johnson, R. S.** (2007). Hypoxia: a key regulator of angiogenesis in cancer. *Cancer Metastasis Rev.* **26**, 281-290.
- Liu, Y., Cox, S. R., Morita, T. and Kourembanas, S.** (1995). Hypoxia regulates vascular endothelial growth factor gene expression in endothelial cells. Identification of a 5' enhancer. *Circ. Res.* **77**, 638-643.
- Lonser, R. R., Glenn, G. M., Walther, M., Chew, E. Y., Libutti, S. K., Linehan, W. M. and Oldfield, E. H.** (2003). von Hippel-Lindau disease. *Lancet* **361**, 2059-2067.
- Ma, W., Tassarollo, L., Hong, S. B., Baba, M., Southon, E., Back, T. C., Spence, S., Lobe, C. G., Sharma, N., Maher, G. W. et al.** (2003). Hepatic vascular tumors, angiectasis in multiple organs, and impaired spermatogenesis in mice with conditional inactivation of the VHL gene. *Cancer Res.* **63**, 5320-5328.
- Maher, E. R. and Kaelin, W. G., Jr** (1997). von Hippel-Lindau disease. *Medicine (Baltimore)* **76**, 381-391.
- Maher, E. R., Iselius, L., Yates, J. R., Littler, M., Benjamin, C., Harris, R., Sampson, J., Williams, A., Ferguson-Smith, M. A. and Morton, N.** (1991). Von Hippel-Lindau disease: a genetic study. *J. Med. Genet.* **28**, 443-447.
- Ober, E. A., Olofsson, B., Makinen, T., Jin, S. W., Shoji, W., Koh, G. Y., Alitalo, K. and Stainier, D. Y.** (2004). Vegf is required for vascular development and endoderm morphogenesis in zebrafish. *EMBO Rep.* **5**, 78-84.
- Oh, H., Takagi, H., Suzuma, K., Otani, A., Matsumura, M. and Honda, Y.** (1999). Hypoxia and vascular endothelial growth factor selectively up-regulate angiopoietin-2 in bovine microvascular endothelial cells. *J. Biol. Chem.* **274**, 15732-15739.
- Ohh, M., Yauch, R. L., Lonergan, K. M., Whaley, J. M., Stemmer-Rachamimov, A. O., Louis, D. N., Gavin, B. J., Kley, N., Kaelin, W. G., Jr and Iliopoulos, O.** (1998). The von Hippel-Lindau tumor suppressor protein is required for proper assembly of an extracellular fibronectin matrix. *Mol. Cell* **1**, 959-968.
- Park, D. M., Zhuang, Z., Chen, L., Szerlip, N., Maric, I., Li, J., Sohn, T., Kim, S. H., Lubensky, I. A., Vortmeyer, A. O. et al.** (2007). von Hippel-Lindau disease-associated hemangioblastomas are derived from embryologic multipotent cells. *PLoS Med.* **4**, e60.
- Pugh, C. W. and Ratcliffe, P. J.** (2003). Regulation of angiogenesis by hypoxia: role of the HIF system. *Nat. Med.* **9**, 677-684.
- Rankin, E. B., Higgins, D. F., Walisser, J. A., Johnson, R. S., Bradfield, C. A. and Haase, V. H.** (2005). Inactivation of the arylhydrocarbon receptor nuclear translocator (*Arnt*) suppresses von Hippel-Lindau disease-associated vascular tumors in mice. *Mol. Cell. Biol.* **25**, 3163-3172.
- Schulte-Merker, S.** (2002). Looking at embryos. In *Zebrafish, a practical approach* (eds C. Nusslein-Volhard and R. Dahm). Oxford: Oxford University Press.
- Schwerte, T., Uberbacher, D. and Pelster, B.** (2003). Non-invasive imaging of blood cell concentration and blood distribution in zebrafish *Danio rerio* incubated in hypoxic conditions in vivo. *J. Exp. Biol.* **206**, 1299-1307.
- Semenza, G. L.** (2001). HIF-1, O(2), and the 3 PHDs: how animal cells signal hypoxia to the nucleus. *Cell* **107**, 1-3.
- Song, M., Yang, H., Yao, S., Ma, F., Li, Z., Deng, Y., Deng, H., Zhou, Q., Lin, S. and Wei, Y.** (2007). A critical role of vascular endothelial growth factor D in zebrafish

- embryonic vasculogenesis and angiogenesis. *Biochem. Biophys. Res. Comm.* **357**, 924-930.
- Stoletov, K., Montel, V., Lester, R. D., Gonias, S. L. and Klemke, R.** (2007). High-resolution imaging of the dynamic tumor cell vascular interface in transparent zebrafish. *Proc. Natl. Acad. Sci. USA* **104**, 17406-17411.
- Tang, N., Mack, F., Haase, V. H., Simon, M. C. and Johnson, R. S.** (2006). pVHL function is essential for endothelial extracellular matrix deposition. *Mol. Cell. Biol.* **26**, 2519-2530.
- Taraboletti, G. and Giavazzi, R.** (2004). Modelling approaches for angiogenesis. *Eur. J. Cancer* **40**, 881-889.
- Thomas, K. A.** (1996). Vascular endothelial growth factor, a potent and selective angiogenic agent. *J. Biol. Chem.* **271**, 603-606.
- Tranos, P. G., Wickremasinghe, S. S., Stangos, N. T., Topouzis, F., Tsinopoulos, I. and Pavesio, C. E.** (2004). Macular edema. *Survey Ophthalmol.* **49**, 470-490.
- Van Poppel, H., Nilsson, S., Algaba, F., Bergerheim, U., Dal Cin, P., Fleming, S., Hellsten, S., Kirkali, Z., Klotz, L., Lindblad, P. et al.** (2000). Precancerous lesions in the kidney. *Scand. J. Urol. Nephrol. Suppl.* **205**, 136-165.
- van Rooijen, E., Voest, E. E., Logister, I., Korving, J., Schwerte, T., Schulte-Merker, S., Giles, R. H. and van Eeden, F. J.** (2009). Zebrafish mutants in the von Hippel-Lindau tumor suppressor display a hypoxic response and recapitulate key aspects of Chuvash polycythemia. *Blood* **113**, 6449-6460.
- Vogel, A. M. and Weinstein, B. M.** (2000). Studying vascular development in the zebrafish. *Trends Cardiovasc. Med.* **10**, 352-360.
- Vortmeyer, A. O., Gnarr, J. R., Emmert-Buck, M. R., Katz, D., Linehan, W. M., Oldfield, E. H. and Zhuang, Z.** (1997). von Hippel-Lindau gene deletion detected in the stromal cell component of a cerebellar hemangioblastoma associated with von Hippel-Lindau disease. *Hum. Pathol.* **28**, 540-543.
- Wanebo, J. E., Lonser, R. R., Glenn, G. M. and Oldfield, E. H.** (2003). The natural history of hemangioblastomas of the central nervous system in patients with von Hippel-Lindau disease. *J. Neurosurg.* **98**, 82-94.
- Westerfield, M.** (1995). *The Zebrafish Book. A Guide for the Laboratory Use of Zebrafish (Danio rerio)*. Eugene, OR: University of Oregon Press.
- Wittenberg, J. B. and Wittenberg, B. A.** (1974). The choroid rete mirabile of the fish eye. I. Oxygen secretion and structure: comparison with the swimbladder rete mirabile. *Biol. Bull.* **146**, 116-136.
- Wong, W. T., Agron, E., Coleman, H. R., Reed, G. F., Csaky, K., Peterson, J., Glenn, G., Linehan, W. M., Albert, P. and Chew, E. Y.** (2007). Genotype-phenotype correlation in von Hippel-Lindau disease with retinal angiomatosis. *Arch. Ophthalmol.* **125**, 239-245.
- Yancopoulos, G. D., Davis, S., Gale, N. W., Rudge, J. S., Wiegand, S. J. and Holash, J.** (2000). Vascular-specific growth factors and blood vessel formation. *Nature* **407**, 242-248.
- Zagzag, D., Krishnamachary, B., Yee, H., Okuyama, H., Chiriboga, L., Ali, M. A., Melamed, J. and Semenza, G. L.** (2005). Stromal cell-derived factor-1alpha and CXCR4 expression in hemangioblastoma and clear cell-renal cell carcinoma: von Hippel-Lindau loss-of-function induces expression of a ligand and its receptor. *Cancer Res.* **65**, 6178-6188.
- Zagzag, D., Lukyanov, Y., Lan, L., Ali, M. A., Esencay, M., Mendez, O., Yee, H., Voura, E. B. and Newcomb, E. W.** (2006). Hypoxia-inducible factor 1 and VEGF upregulate CXCR4 in glioblastoma: implications for angiogenesis and glioma cell invasion. *Lab. Invest.* **86**, 1221-1232.
- Zon, L. I. and Peterson, R. T.** (2005). In vivo drug discovery in the zebrafish. *Nat. Rev. Drug. Discov.* **4**, 35-44.